RSC Advances

# Encapsulation of Therapeutic Lavender Oil in an Electrolyte Assisted Polyacrylonitrile Nanofibres for Antibacterial Applications



| | |
|---|---|
| Journal: | *RSC Advances* |
| Manuscript ID: | RA-ART-08-2014-009425.R1 |
| Article Type: | Paper |
| Date Submitted by the Author: | 25-Sep-2014 |
| Complete List of Authors: | KANDASUBRAMANIAN, BALASUBRAMANIAN; DIAT(DU), MATERIALS ENGINEERING<br>Kodam, Kisan; University of Pune, Chemistry |
| | |

# RSC Advances

## An international journal to further the chemical sciences


*RSC Advances* is an international, peer-reviewed, online journal covering all of the chemical sciences, including interdisciplinary fields.

The **criteria for publication** are that the experimental and/ or theoretical work must be **high quality**, **well conducted** and **demonstrate an advance by adding to the development of the field**.

***RSC Advances* 2013 Impact Factor* = 3.7**

Thank you for your assistance in evaluating this manuscript.

## Guidelines to the referees

Referees have the responsibility to treat the manuscript as confidential. Please be aware of our Ethical Guidelines, which contain full information on the responsibilities of referees and authors, and our Refereeing Procedure and Policy.

**It is essential that all research work reported in *RSC Advances* is well-carried out and well-characterised. There should be enough supporting evidence for the claims made in the manuscript.**

***When preparing your report, please:***

- comment on the originality and scientific reliability of the work;
- comment on the characterisation of the compounds/materials reported - has this has been accurately interpreted and does it support the conclusions of the work;
- state clearly whether you would like to see the article accepted or rejected and give detailed comments (with references, as appropriate) that will both help the Editor to make a decision on the article and the authors to improve it.

***Please inform the Editor if:***

- there is a conflict of interest
- there is a significant part of the work which you are not able to referee with confidence
- the work, or a significant part of the work, has previously been published
- you believe the work, or a significant part of the work, is currently submitted elsewhere
- the work represents part of an unduly fragmented investigation.

**For further information about *RSC Advances*, please visit: www.rsc.org/advances or contact us by email: advances@rsc.org.**

*Data based on 2013 Journal Citation Reports®, (Thomson Reuters, 2014).

## Justification

Our aim is to fabricate a novel composition of polymer and additive in the form of nanofibres. Polyacrylonitrile loaded with lavender oil are electrospun using electrolyte to tailor the nanofibre morphology. Further the chemistry between PAN and the essential components of lavender oil were studied via modelling. Biological tests such as *in-vitro* cytotoxicity, *in-vitro* antibacterial assay and *in-vitro* drug release study are extensively investigated. PAN/Lavender oil nanofibres posses cyto-compatibility, antibacterial property, drug eluting capability and thermal stability.

## REPLY TO EDITORIAL COMMENTS

**Query -1**

**• A suitably revised manuscript in native format (.DOC or TeX) with high quality embedded figures**

**OR**

**• A suitably revised manuscript in native format (.DOC or TeX) with numbered figures, as separate files in .TIF, or .EPS format, with resolution of 600 dpi or greater and schemes preferably as ChemDraw files. Chemwindow files (filename.cwg, filename.cw2), ISIS/Draw exported as sketch format (filename.skc) and ChemSketch exported in ChemDraw format (filename.cdx) may also be supplied. Providing the original figure and scheme files in their native formats will assist us in ensuring the best quality production of your article.**

Response- 1

A separate file of the manuscript has been uploaded in .docx format, which includes the main text with embedded figures, tables and figure captions. Each figure in TIF with 600 dpi has been uploaded separately, as per the suggestion.

**Query-2**

**• A table of contents entry. This should include:**

*** Colour graphic: maximum size 8 cm x 4 cm**

*** Text: one sentence, of maximum 20 words, highlighting the novelty of the work**

Response

A separate file has been uploaded which contains a coloured graphical abstract with 600 dpi resolution and a highlighting sentence.

**Query 3**

**• Suitably revised Electronic Supplementary Information (if any)**

Response:

There is no any supplementary information to be provided for the present manuscript

**Query 4**

**• Suitably revised CIF(s) and corresponding Check CIF reports (if necessary).**

Response:

CIFs and reports are not required for the present manuscript.

**Query 5**

**• A response to the comments made by the reviewer(s). You should also document any changes you have made to the original manuscript. In order to expedite the processing of the revised manuscript, please be as specific as possible in your response to the reviewer(s).**

Response:

Responses to the reviewers' comments are given following the response to editorial comments.

Changes made by authors have been highlighted in the original manuscript.

**Query 6**

**• A PDF version of your revised manuscript including figures, suitable for publication online as an Accepted Manuscript (no highlighting, track changes etc)**

Response:

A PDF version of revised manuscript including figures has been uploaded for publication as accepted manuscript.

## Response to Reviewers Comments

**REVIEWER 1**

**Authors have made a considerable effort to respond to reviewers' comments and I am pleased to recommend acceptance subject to one minor but very important point to the readers, i.e. this work should be put into context with respect to the state-of-the-art. Therefore, I have edited below their first paragraph and I suggest this as a mandatory revision**

Dear Reviewer, Thanks a lot for your valuable suggestions for our paper. As per your suggestion, we have incorporated the necessary changes in the main manuscript and highlighted as well.

Various modern techniques have been employed by various researchers for the preparation of nano-fibres like Centrifugal spinning, solution/melt blowing, pressurized gyration, template synthesis, drawing, phase separation, Self assembly and force assembly. Though, centrifugal spinning is a well known technique to generate homogeneous nanofibres from poorly electrospinnable materials[15-16], but this process is limited by complex spinneret design which leads to large differences in fibre quality and productivity but combining centrifugal motion with another parameters like pressure can be very attractive proposition[17]. On the other side, solution/melt blowing has the capacity to form web of polymeric fibres on a large scale, but it produces fibres in micrometer range[18-19]. At the present time Electrospinning has emerged as a efficacious and facilitating nanotechnology process for creation of seamless nanofibres of varying morphologies from an assortment of polymers, polymer blends and composites[20-21]. The following table (Table 1) contrasts the advantages and disadvantages of electrospinning technique with the other techniques presently employed. Formation of long, continuous fibres, control on the fibre dimension, repeatability and scope of scaling up have provoked us for choosing electrospinning along with its simplicity and suitability for polyacrylonitrile [22-23].

RSC Advances

Cite this: DOI: 10.1039/c0xx00000x

www.rsc.org/xxxxxx

PAPER

# Encapsulation of Therapeutic Lavender Oil in an Electrolyte Assisted Polyacrylonitrile Nanofibres for Antibacterial Applications

**Balasubramanian K.[a*], Kisan M. Kodam[b]**

***Received (in XXX, XXX) Xth XXXXXXXXX 20XX, Accepted Xth XXXXXXXXX 20XX***
**DOI: 10.1039/b000000x**

Electrospinning, a feasible nanotechnology was exploited to engineer Polyacrylonitrile (PAN) nanofibrous mats inclosing a representative hydrophobic drug like essential oil of lavender. Incorporation of electrolytic solution (NaCl) to polymer solution enhanced the electrospinning capability and concentration as small as 0.3% (w/w) of electrolyte resulted in significant nanofibre morphologies, reduced average fibre diameter (88.44nm) and narrow degree of polydispersity. Dosage of drug loaded in PAN nanofibres were varied from 12.5 to 200µg/mL and their cytotoxicity against mouse fibroblast NIH/3T3 were studied *in-vitro*. The antibacterial proficiency was gauged by challenging the materials against *Staphylococcus aureus* and *Klebsiella pneumoniae* bacteria. The PAN nanofibres exhibited effective bactericidal property of 14-15 mm zone of inhibition in at least 8 hr and it remained unaltered over 30 days. The *in-vitro* release of the drug resulted in a dual drug release profiles with initial burst as well as the diffusion dominated release, ensuing enduring antibacterial activity. Incorporation of lavender oil improved the thermal stability resulting in 20% residual mass at $800^0$C, values add to the nanofibres. Modelling of the interactions between PAN and major antimicrobial components of lavender was performed to understand the chemistry between the additive and polymer. Thus PAN nanofibres can be used as a promising antibacterial material in various fields like biomedical, textile and water treatment applications.

## 1. Introduction

Polymer nanofibres hold extensive potential in various applications like electronics, optical devices, batteries and filtration[1-9], due to their exclusive properties such as high surface area-to-volume ratio, tailored fiber morphology and designed porosity, athleticism for physical/ chemical functionalization, drug carrying competency etc. The future scope of these nanofibres can be envisioned in applications like protective materials, technical textiles, medical, filtration, agriculture, automobile, energy [10-13]. An un-ceasing demand of more reliable, robust, consistent and cost effective nanofibres have led to the focus of research on the current state of art[14].

Various modern techniques have been employed by various researchers for the preparation of nano-fibres like Centrifugal spinning, solution/melt blowing, pressurized gyration, template synthesis, drawing, phase separation, Self assembly and force assembly.

[*a] *Department of Materials Engineering, DIAT (DU), Girinagar, Pune, Maharashtra, Ministry of Defence, Email: meetkbs@gmail.com, Fax: (020) 2438-9509, Tel (020) 2438-9680);*

[b] *Department of Chemistry, Savitribai Phule Pune University , Pune – 41100, INDIA*

Though, centrifugal spinning is a well known technique to generate homogeneous nanofibres from poorly electrospinnable materials[15-16], but this process is limited by complex spinneret design which leads to large differences in fibre quality and productivity but combining centrifugal motion with another parameters like pressure can be very attractive proposition[17]. On the other side, solution/melt blowing has the capacity to form web of polymeric fibres on a large scale, but it produces fibres in micrometer range[18-19]. At the present time Electrospinning has emerged as a efficacious and facilitating nanotechnology process for creation of seamless nanofibres of varying morphologies from an assortment of polymers, polymer blends and composites[20-21]. The following table (Table 1) contrasts the advantages and disadvantages of electrospinning technique with the other techniques presently employed. Formation of long, continuous fibres, control on the fibre dimension, repeatability and scope of scaling up have provoked us for choosing electrospinning along with its simplicity and suitability for polyacrylonitrile [22-23].

Antimicrobial resistance is a ticking time bomb which requires swift responsiveness to safeguard the destructive scenario. The use of antibiotic drugs like gentamycin[21], ciprofloxacin[24], polymer norfloxacin[25]etc. to improve the antimicrobial property in polymer is a prominent contribution and an innovative initiative by industries to defence against bacterial colonization. Natural products derived from plants are also known drugs for their therapeutic benefits since antiquity. On the account of their

abundant availability, biocompatibility, low toxicity, green and eco-friendly approach, recently they are widely used in number of food, pharmaceutical, cosmetic, medicinal application ns. They effectively inhibit wide range of microorganisms and cause fewer side effects than synthetic antimicrobial agents in human[26-27]. The antibacterial membranes of crosslinked PVA embedded *Azadirachta indica* and *Curcuma longa* with egg albumin as crosslinking agent were fabriicated for wound healing applications [28]. Chitosan films were blended with essential oils of two endemic herbs *Thymus moroderi* or *Thymus piperella*. These edible films showed antibacterial activity against several spoilage bacteria and they further enhanced the antioxidant activity of chitosan films [29].

Essential oil of lavender (*Lavendula angustifolia*) is one such vital natural product used in aromatherapy as a holistic relaxant and possesses carminative, antiflatulence, anticolic, and antimicrobial properties [27]. Chitosan based lavender essential oil films as an active food packaging materials was developed with improved antibacterial activity, reduced solubility and water vapour permeability[30].

Polyacrylonitrile (PAN) has been well documented as a precursor of high quality stabilized carbon fibres due to their ladder like structure [31]. It is a significant polymeric material widely used for manufacturing synthetic fibres for protective materials, technical textiles, textiles, filtration membranes, agriculture, automobiles, energy, medical etc.[11]. However, the strong static electricity of PAN is prone to adsorption of dust and microbial organisms. Hwang et al[32] prepared modified montmorillonite intercalated with PAN and reacted with $AgNO_3$. The nanocomposite inhibited the growth of bacteria resulting in zone of inhibition (ZOI) of 13.0-13.6 mm. PAN based activated carbon fibre supported with nano-ZnO exhibited strong antibacterial activity against *S.aureus* and *E. coli* [33]. The strong adsorbing efficacy of PAN was utilized to adsorb silver ions and ovalbumin layer-by-layer demonstrated excellent antibacterial activity[34]. Sun et al.[35] developed PAN nanofibrous membranes in combination with amidoxime functional group with silver nanoparticles for filtration of air or water [36-37].

In this research work, we have utilized the therapeutic lavender oil fabricated in an electrospun PAN nanofiber for antibacterial and drug delivery applications. As in case of nanoparticles, incorporation of the natural products in the form of oil eliminates the need for precursor preparation. However, the non-polar nature of oil challenges the electrospinning capability. Introduction of electrolytic solution in the polymer solution overcomes the difficulty. Although the use of electrolytes during the electrospinning has been already reported [20], the incorporation of electrolyte in natural oils to aid the formation of nanofibres has not been investigated. Further, we have characterized the effects of different concentrations of electrolytic solution on the nanofiber morphology. The cyto–compatibility, release kinetics, thermal stability was also explored. This is the first manuscript modelled the chemical interactions between PAN and active components of lavender oil which reveals functionality of PAN matrix. The enhanced antimicrobial resistance of the nanofibres was investigated against the most common pathogens like *Staphylococcus aureus* and *Klebsiella pneumoniae,* which predominantly colonize in skin and wounds and endanger to human health. Investigation of in-vitro drug release study has been accomplished in a buffer release medium to ensure the drug elution capability. These nanofibres with bactericidal properties finds promising role in biopolymers, textiles, filtration applications such as sanitizing water supplies etc.

**Table 1: Comparison of various electrospinning techniques**

| Fibre manufacturing Process | Scope for scaling up | Repeatability | Control on fibre dimension | Advantages | Disadvantages |
|---|---|---|---|---|---|
| Electrospinning | Yes | Yes | Yes | Long and continuous fibres | Solvent recovery issues, low productivity, jet instability |
| Melt blowing | Yes | Yes | Yes | Long and continuous fibres, high productivity, free from solvent recovery issues | Polymer limitations, thermal degradation of polymers |
| Template synthesis | No | Yes | Yes | Easy to change diameter by using different templates | Complex process |
| Drawing | No | Yes | No | Simple process | Discontinuous process |
| Phase separation | No | Yes | No | Simple equipments Required | Only work with selective Polymers |
| Self Assembly | No | Yes | No | Easy to get smaller Nanofibres | Complex process |
| Force spinning | Yes | Yes | Yes | Free from very high voltage, eco-friendly | Requirement of high temperature at times |

## 2. Experimental

### 2.1 Materials

Polyacrylonitrile ($M_w$: 150,000, Sigma Aldrich), Dimethyl formamide (DMF, 99.5%, Sigma Aldrich), Phosphate buffer saline (PBS, pH= 7.4, Thomas Baker), lavender oil (*Lavandula angustifolia*, Bhagat Fine Chemicals, Mumbai) were used as received. Bacterial strains of *Staphylococcus aureus* (MTCC-96) and *Klebsiella pneumoniae* (NCIM-5432) were selected as representative of Gram positive and Gram-negative bacteria respectively.

### 2.2 Measurements

The morphology of PAN/Lavender oil nanofibres were investigated by field emission scanning electron microscopy (Carl Zeiss, Germany) at an accelerating voltage of 5 kV and 10 mm working distance and 20 KX magnification. The average fiber diameter was determined from the field emission scanning electron microscopy (FE-SEM) images using ImageJ software, and around 500 fibres were analysed. Thermogravimetric analysis (TGA, Perkin Elmer, STA 6000) at 30 $^oC$ - 800 $^oC$ (20$^oC$/min) were performed to assess the thermal stability after incorporation of lavender oil in PAN nanofibres. Chemical modification of

PAN due to blending with lavender oil was studied using Fourier transform infrared (FTIR) spectrum. The spectrum was recorded between 400 and 4000 $cm^{-1}$ at room temperature on Perkin-Elmer Spectrum BX FTIR system [38]. The FTIR spectrum was recorded for pristine PAN, lavender oil and PAN-lavender oil system. Consistency was ensured by noting average of 60 iterations in spectral scanning.

### 2.3 Electrospinning of PAN nanofibres

The clear solution of 8 wt% PAN in DMF/Lavender oil[20] was placed in 1 mL glass syringe fitted with a metallic needle of 0.45 mm inner diameter. An electrolytic solution of NaCl was added to the polymeric solution at different concentrations (0%, 0.1%, 0.3% w/w). The syringe was fixed horizontally on the infusion syringe pump to control the mass flow rate (Nanomate Electrospinning, Thukral Services, India).The electrode of high voltage power supply was clamped to the metal needle tip, and the flat aluminium collector used as counter electrode was grounded. The feed rate of the solution was 2.05 µL/min, the applied voltage was 7kV, and the tip collector was placed at a distance of 3.5 cm. Electrospun nanofibres were deposited on a grounded stationary metal collector covered with a piece of aluminium foil. The electrospinning apparatus was enclosed in a Plexiglas box, and the electrospinning was carried out at 24 $^oC$ and 45% relative humidity. The collected fibres were dried at room temperature under the fume hood overnight and stored for several days before their analyses[20,39]. Different concentration of lavender oil was added to PAN solution and their viscosity was measured using (Brookefield Viscometer DVII) and the optimized workable composition was used for further studies.

### 2.4 Molecular dynamic simulations

The molecular dynamic simulations between PAN and the active ingredients of lavender oil like linalyl acetate and linalool were performed using Materials Studio 6.0 software. Briefly, the linalyl acetate, linalool molecular systems were geometrical optimized using Forcite module and COMPASS (Condensed Phase Optimized Molecular Potentials for Atomistic Simulation Studies) force fields[40]. Atactic PAN was conformed to its minimum energy using conformers module by random sampling methods. A 3D cubic cell with periodic boundary conditions of 20 X 20 X 20 Å comprising of 5 PAN polymer chains, 2 linalyl acetate and 2 linalool molecules were constructed using amorphous cell module. All the interactions studies were performed under vacuum conditions.

### 2.5 Biological tests

#### 2.5.1 Determination of antibacterial efficacy

Antibacterial assay was carried out by disk diffusion method against Gram-positive and Gram-negative bacteria. The culture medium of the aforementioned organisms was prepared by using Muller Hinton Broth. A single colony of each test strain was grown in the broth solutions for 24 h at 37 $^oC$ in a rotary shaker (200 rpm). The bacteria were harvested by centrifugation at 4 $^oC$ and 5000 rpm for 10 min and then adjusted to an optical density of 0.5 at 600 nm. To 20 mL of autoclaved nutrient agar, one hundred microliters of each bacterium to be tested was added and the media were poured into sterilized Petri plates. The disk shaped samples of PAN loaded with lavender oil nanofibres of different concentrations 50 µg/mL to 200µg/mL were placed in the Petri plates and incubated for 24 h at 37$^oC$ to record the lowest concentration of the compound required to inhibit the growth of the bacteria. Each test was triplicated and the bacterial zone of inhibition was observed after incubation period is reported [21]. The minimum inhibition concentrations (MIC) were determined by dilution agar method as mentioned by Amine et al [41].

#### 2.5.2 *In-vitro* drug release profile

The release fluid medium with pH 7.5 was prepared by dissolving 20.25 g of $KH_2PO_4$ and 4.53 g of NaOH in 2500 mL of distilled water. Lavender oil loaded PAN nanofibres were immersed in release fluid at 37$^oC$ with stirring rate of 100 rpm. The aliquots of release medium (2.0 mL) was withdrawn at a given time interval, and exchanged with fresh release medium. The drug concentration in the release medium was measured with UV-Vis spectroscopy at wavelength of 200-220 nm. The loading amount (LA) (%) and encapsulation efficiency (EE) (%) were calculated through the following relationship[42]:

LA= Weight of lavender oil in PAN nanofibers/ Weight of lavender loaded PAN fibers ×100

EE= Weight of lavender oil in PAN nanofibers/ Weight of lavender oil in feed ×100

The calculation of corrected concentration of the lavender release from PAN nanofibres is based on the following equation:

$$C_c = C_t + \frac{v}{V}\sum_0^{t-1} C_t \quad - \qquad (1)$$

Where, $C_c$ is the corrected concentration at time t, $C_t$ is the apparent concentration at time t, $v$ is the volume of sample taken, and V is the total volume of the release fluid medium. Each *in-vitro* drug release was done in triplicates [43].

The release of the lavender oil from the PAN matrix was fitted to two mathematical model Higuchi and Krosmeyer Peppas model. Higuchi model applied to release of drug from an insoluble matrix based on Fickian Diffusion.

$$Q_t = K\,(t)^{0.5} \qquad (2)$$

Where, $Q_t$ is the amount of drug released in time t and K is the release constant. Drug release from polymeric systems follows the Kromeyer Peppas model.

$$M_t / M\infty = Kt^n \qquad (3)$$

Where, $M_t / M\infty$ is the fraction of drug released in time t, n is the release exponent and k is the release constant.

#### 2.5.3 *In-vitro* Cytotoxicity Test

Cytotoxic potential of the lavender oil was estimated by varying the concentration from 12.5µg/mL to 200µg/mL in PAN solution. The mouse embryonic fibroblasts cell line (NIH/3T3) was obtained from National Centre for Cell Science (NCCS), Pune and grown in Dulbeccos Modified Eagles Medium (DMEM) containing 10% foetal bovine serum (FBS). The cells were maintained at 37$^oC$, 5% $CO_2$, 95% air and 100% relative humidity. The culture medium was changed twice a week and maintenance cultures were passaged weekly.

The monolayer cells were detached with trypsin-ethylenediaminetetraacetic acid (EDTA) to make single cell suspensions and viable cells were counted using a hemocytometer and diluted with DMEM medium containing 5% FBS to give final density of $1x10^5$ cells/mL. One hundred microlitres per well of cell suspension were seeded into 96-well plates at plating density of 10,000 cells/well and incubated to allow for cell attachment at 37 $^oC$, 5% $CO_2$, 95% air and 100% relative

humidity. After 24 h, the cells were treated with serial concentrations of the test samples. They were initially dissolved in dimethyl sulfoxide (DMSO) and an aliquot of the sample solution was diluted to twice the desired final maximum test concentration with serum free medium. Additional four serial dilutions were made to provide a total of five sample concentrations. Aliquots of 100 µL of these different sample dilutions were added to the appropriate wells already containing 100 µL of medium, resulting in the required final sample concentrations. Following sample addition, the plates were incubated for an additional 48 h at 37 $^{o}$C, 5% $CO_2$, 95% air and 100% relative humidity. The medium containing without samples were served as control and triplicate was maintained for all concentrations[44].

The cytotoxicity test was studied by 3-[4,5-dimethylthiazol-2-yl]2,5-diphenyltetrazolium bromide (MTT) assay. Succinate dehydrogenase enzyme used to cleave tetrazolium ring which converts the MTT to an insoluble purple formazan . Therefore, the amount of insoluble formazan produced is proportional to the number of viable cells. After 48 h of incubation, 15 µL of MTT (5mg/mL) in PBS was added to each well and incubated at 37 $^{o}$C for 4h. The medium was then flicked off with MTT and 100 µl of DMSO was used to solubilize the formed formazan crystals. Further, absorbance has been measured at 570 nm using micro plate reader. Calculation of percentage cell viability with respect to control as follows:

Cell viability (%) = Absorbance of Test Sample / Absorbance of control x 100

## 3. RESULTS AND DISCUSSION

### 3.1 Morphology of electrospun PAN/lavender oil Nanofibres

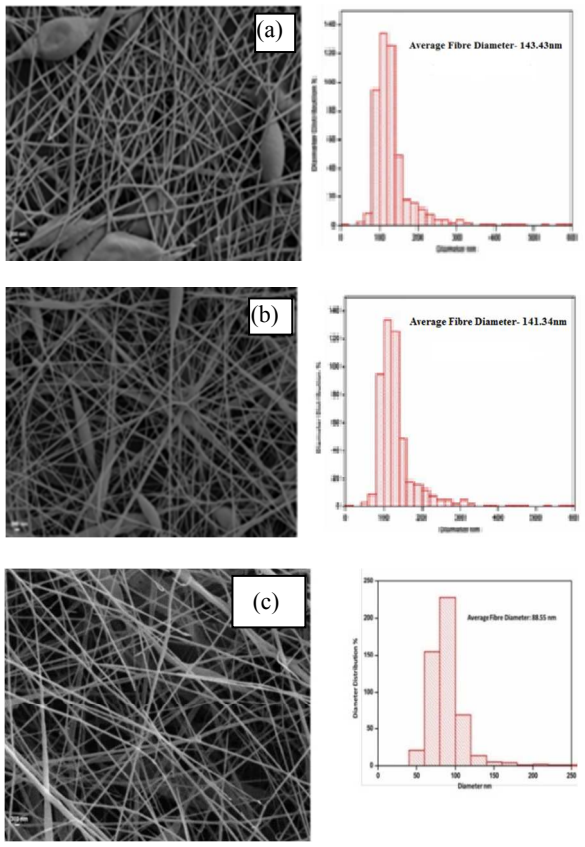


**Fig. 1:** FESEM images of electrospun nanofibres from 8 wt % PAN solution with lavender oil at different concentrations of electrolytic solution: (a) 0 wt% (b) 0.1 wt% and (c) 0.3 wt%. The fibre diameter distributions are shown on the right

The presence of beads on strings is a common problem in the electrospun fibers as they can disturb the unique properties of the fibres, such as decreased specific surface area[45]. Beads on the fibers appeared due to difference in voltage, feed rate and diameter effect. From the solution properties as summarised in Table: 2, it is observed that the solution viscosity increased with the dosage of the lavender oil. For the aforementioned processing parameters, the workable viscosity was for 100 µg/mL, dosage and the morphology details of this concentration are reported hence forth. The morphologies of electrospun nanofibres obtained from homogenous solution of PAN and lavender oil with addition of electrolytic solution 0%, 0.1% and 0.3% (w/w, with respect to PAN) and the representative histograms of fibre diameter distribution are shown in Figure 1 with maintained processing parameters ( PAN/ Lavender- 8wt%, voltage-7kV, feedrate-2.05µg/mL and distance- 3.5cm). Regular PAN/Lavender oil nanofibres with an average fibre diameter (AFD) of about 143.4 nm are evident from Figure 1. However, due to the instability of the jet at the spinning tip, a few shuttle shaped beads were found to be coalesced and cohered with uniform nanofibres. With the addition of 0.1% electrolytic solution the morphology of the beads showed a substantial change with negligible decrease in AFD. The bead formation eventually disappeared and fine nanofibres of AFD 88.55 nm was obtained due to increase in conductivity of the solution by adding 0.3% electrolytic concentration[46]. Further the degree of polydispersity of the nanofibres reduced due to the addition of electrolytic solution. Wright et al.[37] has utilized NaCl mandrel above the rotating collection mandrel for improved porosity in electrospun PLLA scaffolds. Tromp et al. [47] added 0.5 M NaCl solution during the electrospinning of polysaccharides, and observed that the jet formed from the solution was not focussed as in the case of polymer solution without electrolyte resulting in the deposition of fibres all over the collecting plate. Hence the incorporation of electrolytic solution in the PAN/Lavender solution has improved the nanofibres morphologies of PAN blended with non-polar oil, and this suggests that the jet instability increased in the presence of salt. Thus, the results showed, by addition of electrolytic solution influenced bead morphology, AFD and the degree of polydispersity of the nanofibres due to the increase in polarity of the polymer solution.

**Table 2: Summary of Solution Properties Used in the Experiment**

| Dosage of oil (µg/mL) | Viscosity (mPa s) |
|---|---|
| 0 | 491.2 |
| 25 | 493.4 |
| 50 | 506.2 |
| 100 | 513.2 |
| 200 | 520.3 |

### 3.2 Thermal stability of PAN

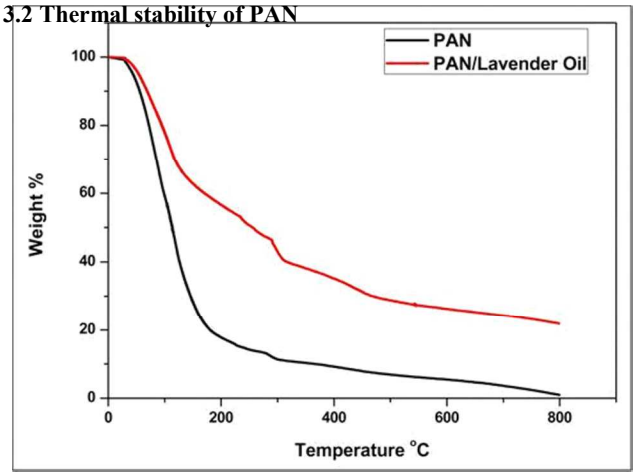


**Fig. 2**: TGA of PAN and PAN/Lavender oil

Figure 2 shows the TGA curve of PAN and PAN with lavender oil was recorded in an inert atmosphere ($N_2$). Each sample exhibits distinguishing thermal degradation process. The thermal degradation curve of PAN exhibits two stage decomposition. The first mass loss begins around 100-200°C and was associated with nitrile oligomerization, which produces volatile products such as $NH_3$, HCN, $CH_3CN$ etc., resulting in residual mass of ca. 20% [48]. The second stage degradation occurs around 270-300°C and was allied with the thermal degradation reaction of the polymer resulting in mass loss of ca. 10% and the final degradation occurs around 790°C. The TGA curves of the PAN/Lavender reveals four thermal degradation steps. The first step occurs in low temperature region (100-150°C) and second, third and fourth stages mass loss occurs around 150-310 °C, 310-470 °C and 470-800°C resulting in a residual weight % of ca. 20%. This indicates that the physisorbed or immobilized lavender oil in the PAN possibly fills the amorphous domains of the polymers and thereby increasing the residual masses compared to pristine PAN. Thus the thermal destruction of the PAN nanofibres has been significantly improved by the immobilization of lavender oil.

### 3.3 FTIR analysis

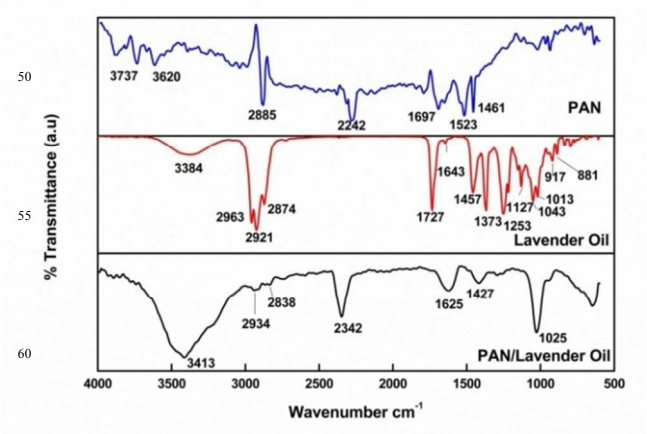


**Fig. 3**: FTIR spectrum of PAN, Lavender oil and PAN/Lavender oil

The FTIR spectroscopy was performed to elucidate the chemical modifications due to addition of lavender oil to PAN (Figure 3). In the spectrum of PAN peak at 2242 $cm^{-1}$ corresponds to the C≡N group. Further the bands at 2881 $cm^{-1}$ and 1461 $cm^{-1}$ correspond to the stretching and bending vibrations of C-H bonds [49].

In the spectrum of lavender oil, a broad peak at 3384 $cm^{-1}$ corresponding to an O-H stretch indicate the presence of alcohol. The strong bands related to C=O (1727 $cm^{-1}$) and C-O (1253 and 1127 $cm^{-1}$) indicated the stretching of ester groups present. Bands at 2963 and 1643 $cm^{-1}$ are associated with C=C stretching, while 1013, 917, 881, 690 $cm^{-1}$ can be assigned to C-H deformations. Stretching of methyl (2921 and 2874 $cm^{-1}$) and methylene groups (2963 $cm^{-1}$) are indicated by strong bands in the spectrum, in addition to bending (1457 and 1373 $cm^{-1}$). The bands in the FTIR spectrum of lavender oil are same as those predicted by other authors [50-51].

The results of PAN with lavender oil shows that the numbers of peaks in the spectrum are reduced. The broad peak corresponding to O-H and band associated with nitrile group is still present; however the bands corresponding to C-H stretching of methyl and methylene groups are affected. The strong peak at 1727 $cm^{-1}$ assigned to the ester C=O stretch observed in lavender oil spectrum appears as short band at 1625 obscuring the peaks of C=C. Bands associated to C-H deformations are no longer present. Appearance of strong peak 1025 $cm^{-1}$, and broad peak at 3413 $cm^{-1}$ corresponds to the primary amine and H-bonding due to N-H stretch respectively. Thus the spectrum shows the interaction between PAN and lavender oil exists and lavender oil can be immobilized in PAN matrix.

### 3.4 Modelling studies: Interactions of PAN and Lavender oil components

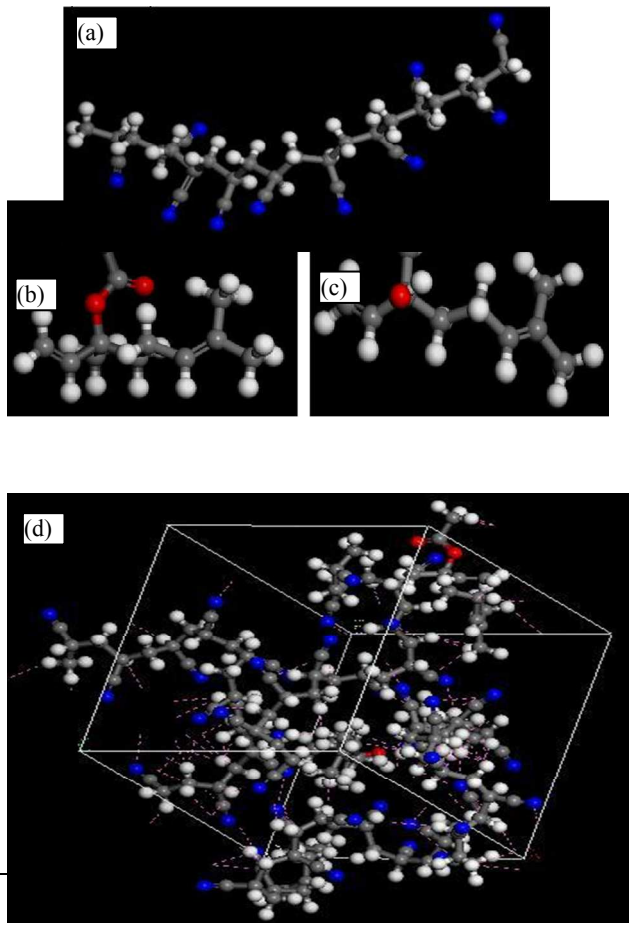

**Fig. 4**: Geometrically optimised molecules (a) Linalyl acetate (b) Linalool (c) PAN (d) Amorphous unit cell of (a),(b), (c) showing the interactions.

The present study envisages the interaction between the major components of lavender oil with PAN using Materials Studio 6.0 software. Initially, the components of lavender oil, linalyl acetate and linalool molecules were constructed in a linear fashion and the geometrically optimized molecules (Figure 4(a) and (b)) resulted in total minimization energy of the system to $E_{Total}$ = -40.97 kcal/mol and $E_{Total}$ = -38.57 kcal/mol respectively. The PAN system was modelled as an ideal macromolecule of 10 repeating units in a linear atactic fashion. The macromolecules were generated with 200 conformations and the geometrically optimized PAN conformer with minimization of total energy $E_{Total}$ = -12.11kcal/mol was calculated as shown in Figure 4(c). A simulated environment was created by constructing three-dimensional cubic unit as shown in Figure 4(d). The interactions between PAN and the lavender molecules yielded no bond formation between them and minimization total energy as $E_{Total}$ = -364.77 kcal/mol, however, achieves the close proximity between PAN/ lavender molecules due to van der waal forces and the electrostatic forces of attraction(Figure 4(d)). This confirms the physisorbed or immobilized behavior of the lavender components encapsulated in the PAN matrix without any chemical interactions. Thus, the minimization in total energy of PAN/lavender components to the total energies of the individual molecules recommends the existence of the system and the physisorption or immobilization of the components proposes the functionality of the PAN matrix as a biopassive surface[52].

### 3.5. Biological tests

#### 3.5.1 *In-vitro* Antibacterial Assay

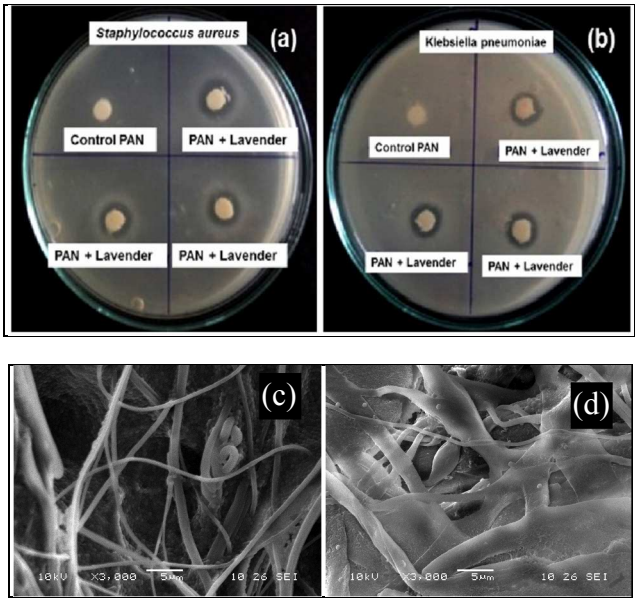


**Fig. 5:** *In-vitro* antibacterial assay against (a) *Staphylococcus aureus* (b) *Klebsiella pneumonia* (c) SEM image of Pristine PAN fibre cultured with bacteria (d) SEM image of PAN/ lavender oil fibre with bacteria

Figure 5(a) and (b) illustrates *in-vitro* antibacterial activity of PAN/Lavender oil (100 µg/mL), against the Gram-positive and Gram-negative bacteria by exposing a clear zone of inhibition (ZOI). PAN used as a control in the assay does not exhibit any ZOI. PAN/Lavender oil revealed ZOI measuring ca. 14-15 mm against both the pathogens after an incubation period of 24 h with MIC of 100µg/ml. The ZOI remained unaltered for more than 30 days, which signifies sustained antibacterial activity of the system. Other concentrations 12.5, 25 and 50 µg/mL were not sufficient to inhibit the bacterial growth. Fig 5 (c) exhibits the SEM image of the pristine PAN fiber, cultured with bacteria, which clearly elucidates the formation of colonies on the surface of PAN fiber. While fig 5 (d), illustrated the significant reduction in the number of bacterial colonies on agar medium of PAN/lavender composite fibers. The antibacterial efficacy of the PAN/lavender fiber can be attributed to the presence of various components in lavender oil like linalool, linalyl acetate, 1,8-cineole, β-ocimene (usually both cis and trans), terpinen-4-ol and camphor[53]. Components with phenolic structure are known to enhance the antimicrobial activity by alkyl substitution into the phenolic nucleus of the microorganisms. The alkylation has been proposed to alter the aqueous and non-aqueous phases including the bacterial phase and the formed phenoxyl radical which interacts with the species. The presence of electronegative compounds like acetate, aldehyde, terpenoid moieties are known to enhance the antimicrobial activity of the parent compound. These compounds interfere in the biological processes involving electron transfer, protein translocation, phosphorylation steps, and other enzyme dependent reactions and therefore inhibit the growth of the microorganism. Their site of action appeared to be at the phospholipids bilayer formed by the biochemical mechanisms of the cell [54].

#### 3.5.2 Lavender loading and *In-vitro*

**Table 3:** Properties of PAN/ Lavender nanofibers

| Samples | Loading amount (%) | Encapsulation efficiency (%) |
|---|---|---|
| 0.1 wt% PAN/ Lavender | 8.2 | 25.8 |
| 0.2 wt% PAN/ Lavender | 10.4 | 28.4 |
| 0.3 wt% PAN/ Lavender | 13.6 | 32.4 |

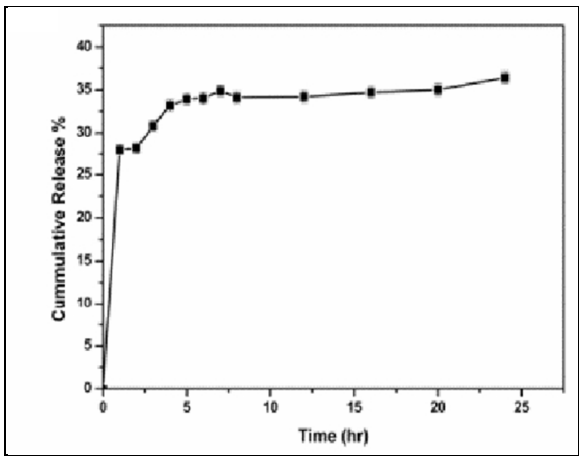


**Fig.6**: *In-vitro* release study of Lavender oil from PAN film for 24 h

The encapsulation efficiency and loading amount of different concentration of lavender oil encapsulated in PAN nanofibers were presented in Table 3. 0.3wt% lavender oil encapsulated in PAN reveals the high loading content as 13.6%. Both loading amount and encapsulation efficiency were increased with increasing the lavender oil wt% in the matrix[42].

To mimic the internal biological environment, the *in- vitro* drug release of lavender oil from the PAN matrix was studied in a buffer release medium (pH 7.4). The release was monitored by UV-vis spectroscopy for 24 h at 296 nm under ambient conditions (Figure 6). It is elucidated from fig 8.that 27% of oil was released within 2 h which can be attributed to the initial burst of loosely bounded oil particles to the PAN fibre surface[28]. In many cases, the initial release increases with increasing lavender oil loading [42]. Further, a controlled release was observed up to 24 h, resulting in a cumulative release of 38%. The lavender oil is physisorbed in the PAN matrix as observed in modelling studies are released by diffusion from the core to the surrounding [55-56]. Thus, the cumulative release of lavender oil from PAN clearly indicates the diffusion is a two-step release profile of initial burst followed by controlled diffusion.

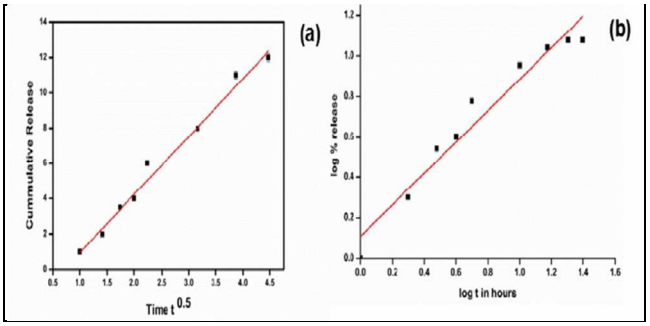


**Fig.7**: *In-vitro* release data fitted to (a) Higuchi model (b) Krosmeyer-Peppas model

The release kinetics was fitted to Higuchi and Krosmeyer Peppas model as expressed in Figure 7. The regression coefficient values ($R^2$) were obtained as 0.9891 and 0.9462 while $K_H$ = 3.286 (Figure 7b) was fitted to release kinetics. The $R^2$ values clearly indicate the release profile of lavender oil best fits to Higuchi model which signifies the hydrophobic drug release from an insoluble matrix [57].

### 3.5.3 *In-vitro* cytotoxicity assay

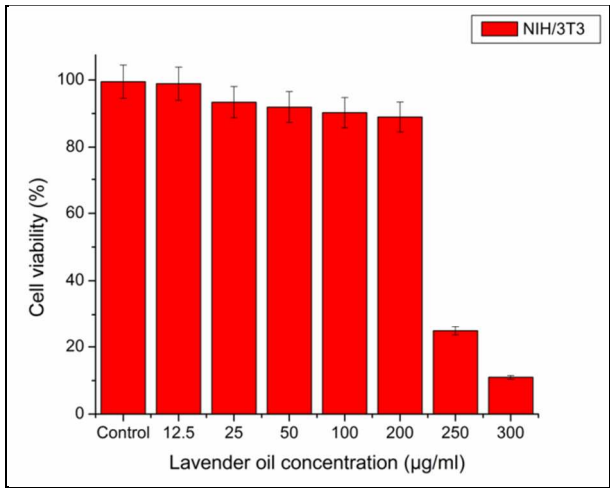


**Fig. 8:** MTT Assay results of mouse fibroblast NIH/3T3 cells exposed to lavender oil at different concentrations

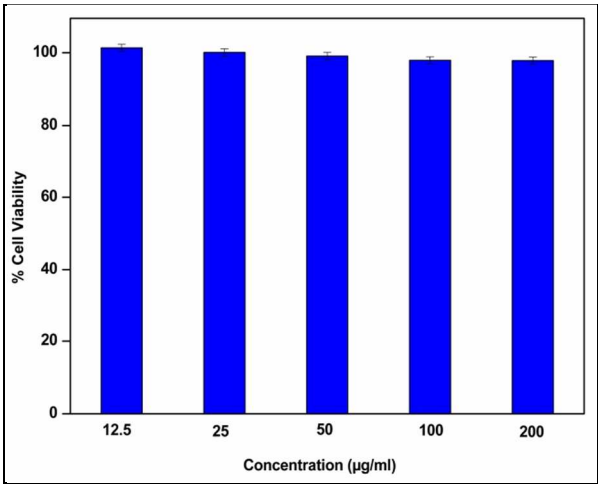


**Fig. 9:** MTT assay results of mouse fibroblast NIH/ 3T3 cells to exposed to PAN blended with lavender oil at different concentrations

An ideal PAN nanofiber for biomedical applications should exhibit cytocompatibility which was ascertained through *in-vitro*

cytotoxicity tests via MTT assay. Figure 8 & 9 shows the cytotoxicity results of the cell lines exposed to lavender oil and PAN/lavender oil for 48 h with an increasing concentration. The cell viability of NIH/3T3 cells after incubation in the medium containing various concentrations of lavender oil and PAN/ lavender oil in the range of 0- 300 and 0-200μg/mL. PAN/lavender oil shows 90-100 % cell viability. Evan et al.[58] studied on cytotoxicity of lavender oil on human skin cells demonstrates damage to skin membranes at concentration of 0.25% v/v. However in the present system, PAN nanofibres acts as a carrier vehicle for lavender oil, and precludes cell damage even at higher concentration of 200 μg/mL.

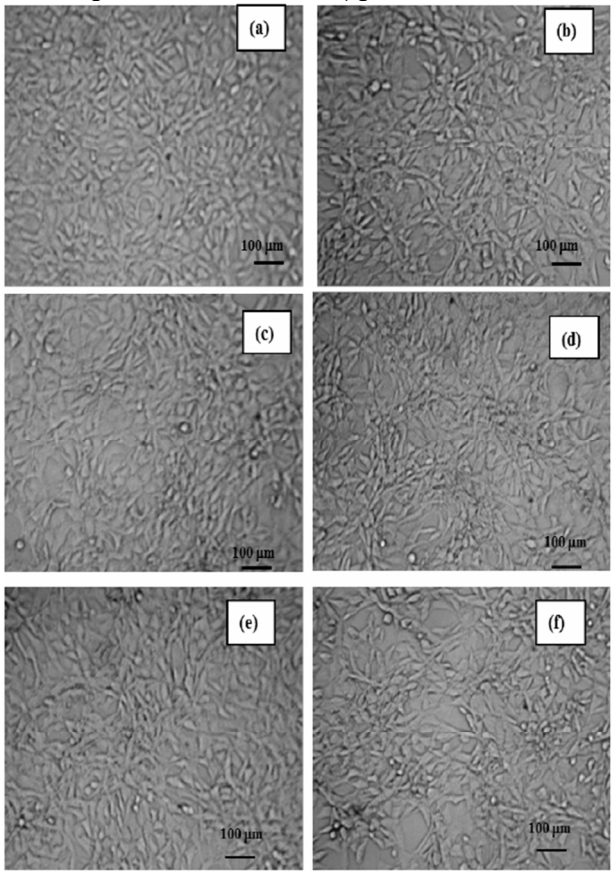


**Fig.10:** Photomicrograph of mouse fibroblast NIH/3T3 cell lines after treatment with samples at concentrations of lavender oil for 48 h (a) Control (b) 12.5 μg/mL (c) 25 μg/mL (d) 50 μg/mL (e) 100 μg/mL (f) 200 μg/mL.

The photomicrographs of the NIH/3T3 cell lines after treatment with control (PAN) and PAN/lavender oil samples has been illustrated in Figure 10. Interestingly, the cell morphology observed in control and drug loaded samples remains same and does not exhibit a change in size or appearance of cellular components or disruption in their configuration. Further, some of the cells were found dead when PAN fibers are cultured with 200μg/mL of lavender oil. The qualitative and quantitative study justifies the cytocompatibility of all the PAN samples with different concentration of lavender oil.

## 4. Conclusions

The goal of this study is to develop an electrospun PAN/ lavender oil nanofibers for antibacterial applications. An increase in the additive concentration of electrolytic solution of NaCl from 0.1 to 0.3% in PAN/ Lavender oil solution leads to drastic enhancement in the fiber morphology. A reduction in average fiber diameter was observed from 143.4 nm to 88.55 nm with addition of 0.3 w/w% of NaCl solution. In addition to this, reduction in degree of polydispersity was also observed. Thus, addition of electrolytic solution in PAN solution increased the likelihood of incorporating therapeutic oils in nanofibres. The modelling study confirms the biopassive nature of PAN matrix due to physisorption behavior / immobilization of active components of lave3nder. An improved thermal stability was observed due to the incorporation/ immobilization of lavender oil in PAN nanofibres, which is further confirmed by an appearance of a strong/ broad peak at 1025 and 3413cm$^{-1}$ in the FT-IR spectrum. The pharmacological studies show that 100% cell viability was depicted till 200μg/mL reveals the non-cytotoxic nature of therapeutic nanofibres to mouse fibroblast. The zone of inhibition (13-14mm) was unchanged for 30 days signifies sustained antibacterial property (MIC: 100μg/mL). The drug release kinetics best fitted to Higuchi model and in- vitro dual profile of the system provides 38% net release within 24hr. Further, these nanofibers can be fabricated to advanced morphologies like porous, core and shell, nanofibers carrying encapsulations and sandwich morphologies using various antimicrobial additives to enhance the sustained drug release and antimicrobial property.

## Acknowledgements

The authors thank Dr. Prahlada, Vice Chancellor DIAT (DU) for his support and encouragement. Financial assistance is from DIAT-DRDO programme on Nanomaterials (EPIPR/ER/100 3883/M/01/908/2012/D (R&D)/1416 Dated: 28.03.2012). We are also grateful to Dr Mukundan, NPOL, DRDO, Cochin for the Materials studio support. Also would like to thanks Premika Govindraj, Dhananjay Gunjal, Nitesh Singh, Ramdayal Yadav and Yutika Badhe for continuous technical support.

### Declaration of Interests

The authors report no declarations of interest.

## Notes and References

[1] S. Chaudhari , M. Srinivasan , J. Mater. Chem. **2012** , *22* , 23049 .
[2] M. Li , J. Zhang , H. Zhang , Y. Liu , C. Wang , X. Xu , Y. Tang , B. Yang , Adv. Funct. Mater. **2007** , *17* , 3650 .
[3] A. A. Sagade , K. Venkata Rao , U. Mogera , S. J. George , A. Datta , G. U. Kulkarni , Adv. Mater. **2012** , *25* , 559 .
[4] V. Vohra , U. Giovanelle , R. Tubino , H. Murata , C. Botta , ACS Nano **2011** , *5* , 5572 .
[5] Y. Li , B. K. Guo , L. W. Ji , Z. Lin , G. J. Xu , Y. Liang , S. Zhang , O. Toprakci , Y. Hu , M. Alcoutlabi , X. W. Zhang , Carbon, **2013** , *51* , 185 .
[6] Y. Li , C. W. Joo , J. Appl. Polym. Sci. **2012** , *126* , E252 .
[7] S. Sinha-Ray , Y. Zhang , A. L. Yarin , Langmuir, **2011** , *27* , 215 .
[8] D. Y. Tu , S. Pagliara , R. Cingolani , D. Pisignano , Appl. Phy. Lett. **2011** , *98* , 023307 .
[9] Y. C. Chiu , Y. Chen , C. C. Kuo , S. H. Tung , T. Kakuchi, W. C. Chen , Appl. Mater. Interface **2012** , *4* , 3387 .
[10] Chen M, Wang C, Fang W, Wang J, Zhang W, Jin G, Diao G. Langmuir, 2013, 29, 11858.
[11] Nataraj SK, Yang KS, Aminabhavi TM. Prog. Polym. Sci.,

2012, 37, 487.
[12] Liu Y, Ma G, Fang D, Xu J, Zhang H, Nie J. Carbohydr. Polym, 2011, 83, 1011.
[13] Li L, Li H, Qian Y, Li X, Singh GK, Zhong L, Liu W, Lv Y, Cai K, Yang L. Int. J. Biol. Macromol., 2011, 49, 223.
[14] C. J. Luo , S. D. Stoyanov , E. Stride , E. Pelan , M. J. Edirisinghe ,Chem. Soc. Rev. **2012** , *41* , 4708 .
[15] L. Wang , J. Shi , L. Liu , E. Secret , Y. Chen , Microelectron Eng. **2011** , *88* , 1718 .
[16] M. R. Badrossamay , H. A. McIlwee , J. A. Goss , K. K. Parker , Nano Lett. **2010** , *10* , 2257 .
[17] S. Mahalingam, M. Edirisinghe, Macrolecular Rapid Communications, 2013, 34, 1134.
[18] E. S. Medeiros , G. M. Glenn , A. P. Klamczynski , W. J. Orts , J. Appl. Polym. Sci. **2009** , *113* , 2322 .
[19] R. G. Zhao , L. C. Wadsworth , Polym. Eng. Sci. **2003** , *43* , 463 .
[20] Thomas V, Donahoe T, Nyairo E, Dean DR., Vohra YK. Acta Biomater., 2011, 7, 2070.
[21] Chen M, Hu M, Wang D, Wang G, Zhu X, Yan D, Sun J. Bioconjugate Chem., 2012, 23, 1189.
[22] Zhou F, Gony R., Polym Int, 2008, 57, 837
[23] Patnaik A, Anandjiwala R, Rengasamy R, Ghosh A, Pal H., Textile Progr, 2007, 39, 67.
[24] Giroud F, Gorgy K, Gondran C, Cosnier S, Pinacho DG, Marco MP, Sanchez-Baeza FJ. Anal. Chem., 2009, 81, 8405–9
[25] Dizman B, Elasri MO, Mathias LJ. Biomacromolecules, 2005, 6, 514.
[26] Islam S, Shahid MF. J. Clean. Prod., 2013, 57, 2.
[27] Yoon C, Moon S, Jeong J, Shin Y, Cho S, Ahn K, Yang J, Kim G. J Asia Pac Entomol., 2011, 14, 411.
[28] Yadav R, Kandasubramanian B. Mater. Lett., 2013, 110, 130.
[29] Ruiz-Navajas Y, Viuda-Martos M, Sendra E, Perez-Alvarez JA, Fernández-López J. Food Control, 2013, 3, 386.
[30] Zhi-hong Z, Yu-yue Q, Jian F, Tian-rui Z,Chun-sheng C. Adv. Mat. Res., 2013, 706, 197.
[31] Rahaman MSA, Ismail AF, Mustafa A. Polym. Degrad. Stab., 2007, 92, 1421.
[32] Hwang JJ, Ma TW. Mater. Chem. Phys., 2012, 136, 613.
[33] Li Q. Chem. Res. Chin. Univ. Chemical, 2013, 29, 1011.
[34] Song R, Yan J, Xu S, Wang Y, Ye T, Chang J. Colloids Surf. B., 2013, 108, 322.
[35] Zhang L, Luo J, Menkhaus TJ, Varadaraju H, Sun Y, Fong H. J. Membr. Sci., 2011, 369, 499.
[36] Wright LD, Andric T, Freeman JW. Mater. Sci. Eng. C, 2011,31, 30.
[37] Heikkila P, Harlin A. Express Polym Lett., 2009, 3, 437.
[38] Wu X-M, Branford-White CJ, Yu D-G, Chatterton NP, Zhu L-M. Colloids Surf., B, 2011, 82, 247.
[39] del Valle LJ, Díaz A, Royo M, Rodríguez-Galán A, Puiggalí J. Express Polym Lett, 2012, 6, 266.
[40] Grujicic M, Cao G, Roy WN. J. Mater. Sci., 2004, 39, 2315.
[41] Amine Dib ME, Allali H, Bendiabdellah A, Meliani N, Tabti . J. Saudi Chem. Soc., 2013, 17, 381.
[42] Zuxiao Yu, Bin He, Chunyan Long, Rong Liu, Mingming Sheng, Gang Wang, James. Z. Tang, and Zhongwei Gu, Macromolecular Research, 2012, 20, 3, 250.
[43] Lancaster S, Kakade S, Mani G. Langmuir, 2012, 28, 11511.
[44] Reinwald Y, Johal RK, Ghaemmaghami AM, Rose FRAJ, Howdle SM., Shakesheff KM. Polymer, 2013, 55, 435.
[45] Li D, Xia Y. Adv Mater 2004;16, 1151–70.
[46] Fong H, Chun I, Reneker D.H. Polymer, 1999, 40, 4585.
[47] Stijnman AC, Bodnar I, Tromp HR. Food Hydrocolloids, 2011, 25,1393.
[48] Korobeinyk AV, Whitby RLD, Mikhalovsky SV. Eur. Polym. J., 2012, 48, 97.
[49] Naraghi M, Arshad SN, Chasiotis I. Polymer, 2011, 52, 1612.
[50] Shellie R, Mondello L, Marriott P, Dugo G. J. Chromatogr. A, 2002, 1-2, 225.
[51]Morgan TJ, Morden WE, Al-Muhareb E, Herod AA, Kandiyoti R. Energy Fuels, 2006, 20, 734.
[52] Chranley M, Textor M, Acikgoz C. React. Funct. Polym. 2011, 71, 329.
[53] Cavanagh HMA, Wilkinson JM. Phytother. Res.,2002,16, 301.
[54] Lis-Balchin M. Taylor & Francis, Newyork, 2002
[55] King WJ, Murphy WL. Polym. Chem., 2011, 2, 476.
[56] Coelho J, Ferreira P, Alves P, Cordeiro R, Fonseca A, Gois J. EPMA J., 2010, 1, 164.
[57] Huang X, Brazel CS., J. Controlled Release, 2001, 73, 121.
[58] Prashar A, Locke IC, Evans CS. Cell Prolif., 2004, 37, 221.

**Figure caption**

**Fig. 1**: SEM images of electrospun nanofibres from 8 wt % PAN solution with lavender oil at different concentrations of electrolytic solution: (a) 0 wt% (b) 0.1 wt% and (c) 0.3 wt%. The fibre diameter distributions are shown on the right

**Fig. 2**: TGA of PAN and PAN/Lavender oil

**Fig. 3**: FTIR spectrum of PAN, Lavender oil and PAN/Lavender oil

**Fig. 4**: Geometrically optimised molecules (a) Linalyl acetate (b) Linalool (c) PAN (d) Amorphous unit cell of (a),(b), (c) showing the interactions.

**Fig. 5**: *In-vitro* antibacterial assay against (a) *Staphylococcus aureus* (b) *Klebsiella pneumonia* (c) SEM image of Pristine PAN fibre cultured with bacteria (d) SEM image of PAN/ lavender oil fibre with bacteria

**Fig. 6**: *In-vitro* release study of Lavender oil from PAN film for 24 h

**Fig. 7:** *In-vitro* relesae data fitted to (a) Higuchi Model (b) Krosmeyer-Peppas Model

**Fig.8:** MTT Assay results of mouse fibrous exposed to lavender oil at different concentrations

**Fig. 9:** MTT Assay results of mouse fibrous exposed to PAN blended with lavender oil at different concentrations

**Fig. 10**: Photomicrograph of NIH/3T3 cell lines after treatment with samples at various concentrations of lavender oil for 48 h (a) Control (b) 12.5 μg/ml (c) 25 μg/ml (d) 50 μg/ml (e) 100 μg/ml (f) 200 μg/ml.

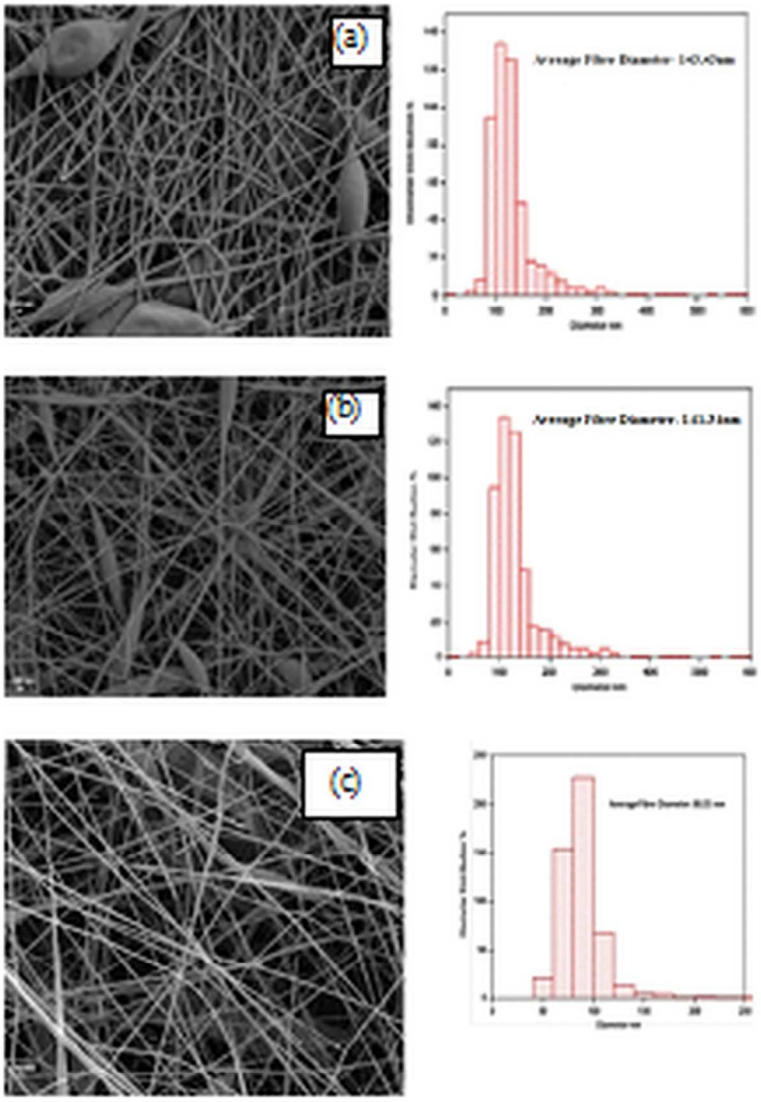


FESEM images of electrospun nanofibres from 8 wt % PAN solution with lavender oil at different concentrations of Fig. 1: FESEM images of electrospun nanofibres from 8 wt % PAN solution with lavender oil at different concentrations of electrolytic solution: (a) 0 wt% (b) 0.1 wt% and (c) 0.3 wt%. The fibre diameter distributions are shown on the right
91x119mm (300 x 300 DPI)

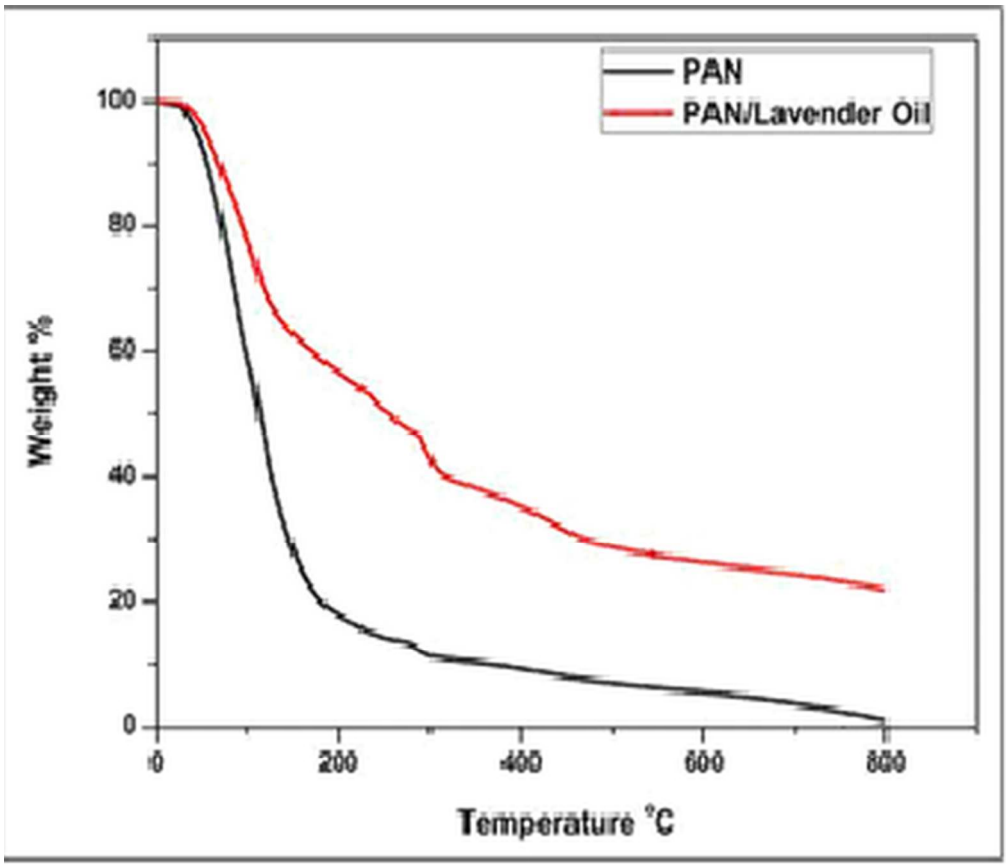


Fig. 2: TGA of PAN and PAN/Lavender oil
76x66mm (300 x 300 DPI)

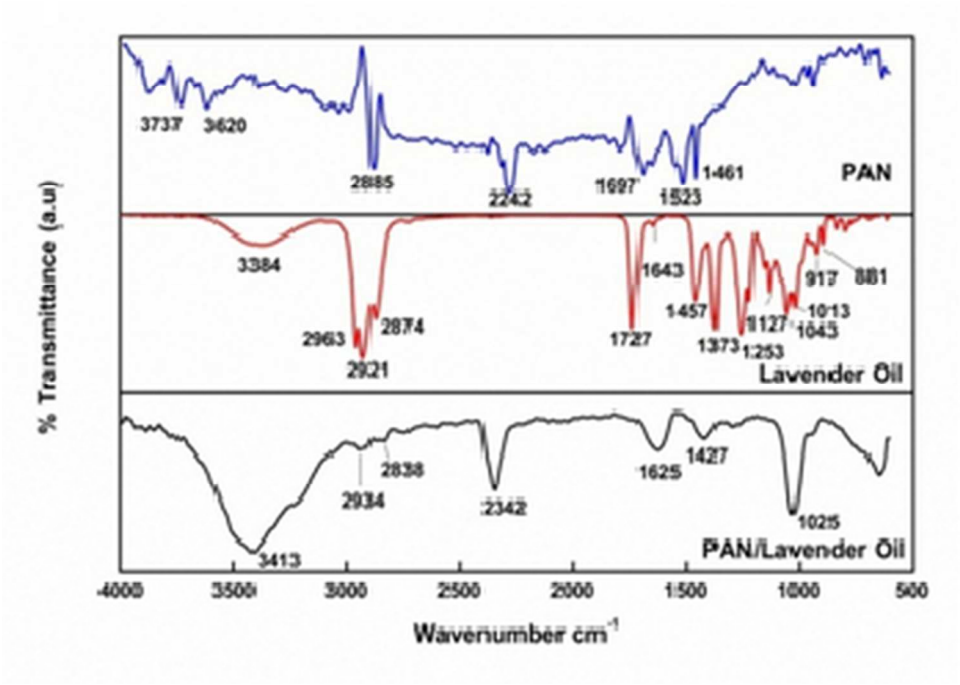


Fig. 3: FTIR spectrum of PAN, Lavender oil and PAN/Lavender oil
67x46mm (300 x 300 DPI)

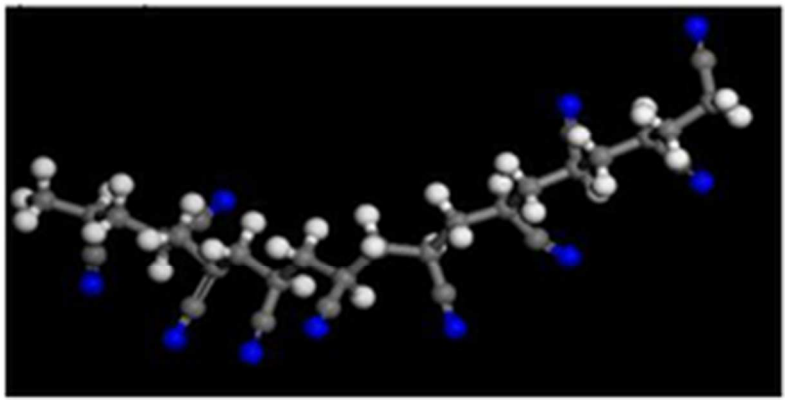

Geometrically optimised molecules (a) Linalyl acetate
33x16mm (300 x 300 DPI)

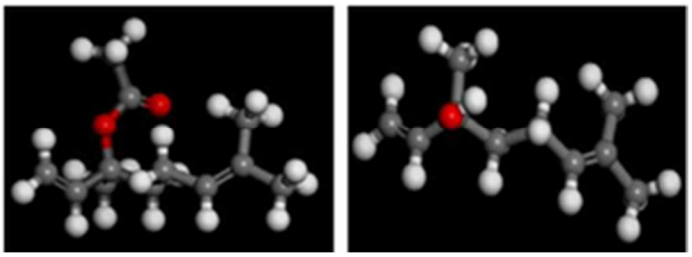

Geometrically optimised molecules (b) Linalool (c) PAN(b), (c) showing the interactions.

29x10mm (300 x 300 DPI)

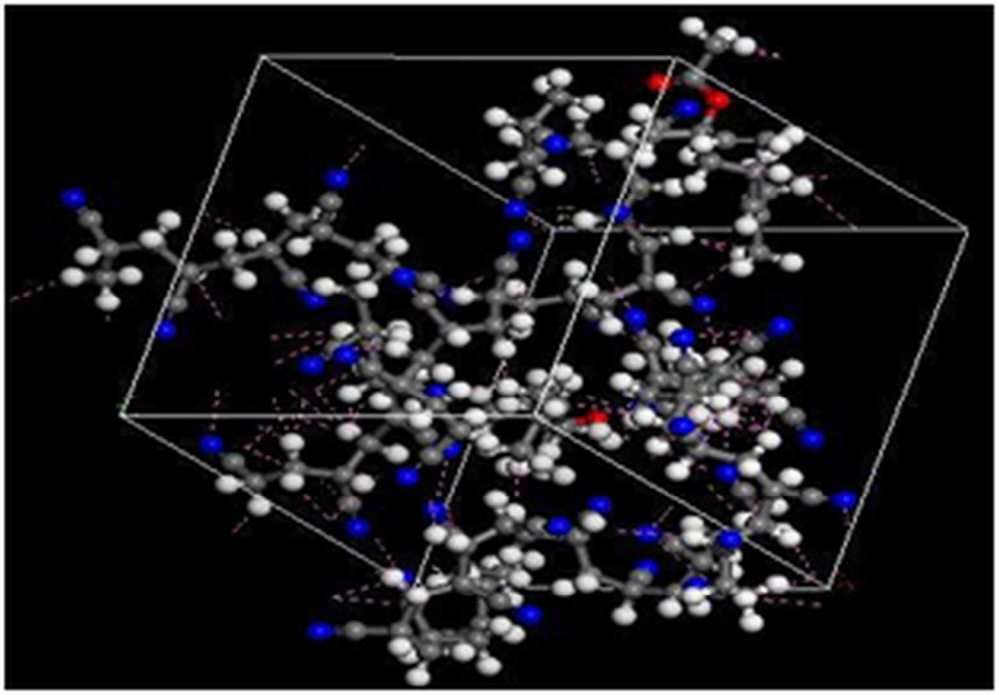

Geometrically optimised molecules (d) Amorphous unit cell

57x40mm (300 x 300 DPI)

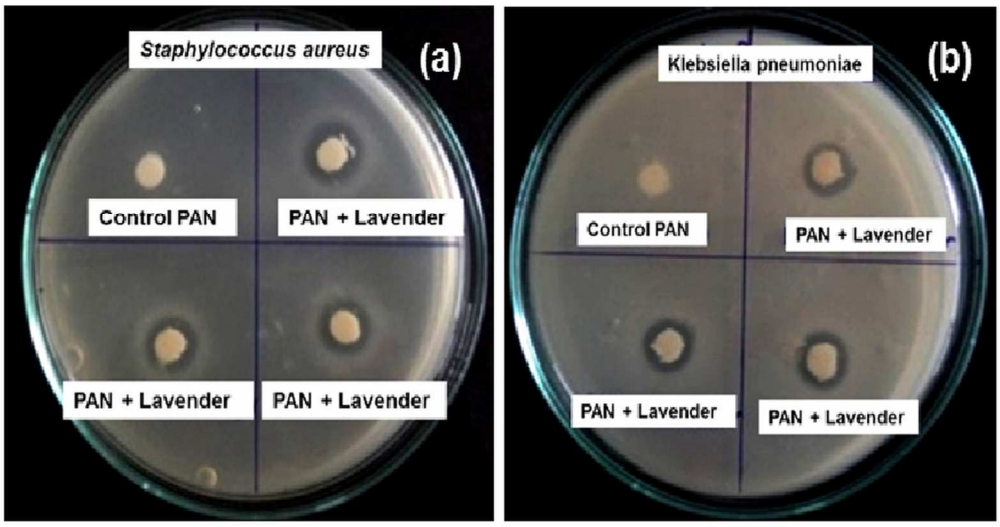


In-vitro antibacterial assay against (a) Staphylococcus aureus (b) Klebsiella pneumonia
120x62mm (300 x 300 DPI)

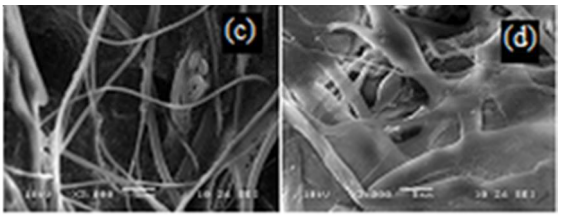


(c) SEM image of Pristine PAN fibre cultured with bacteria (d) SEM image of PAN/ lavender oil fibre with bacteria
23x8mm (300 x 300 DPI)

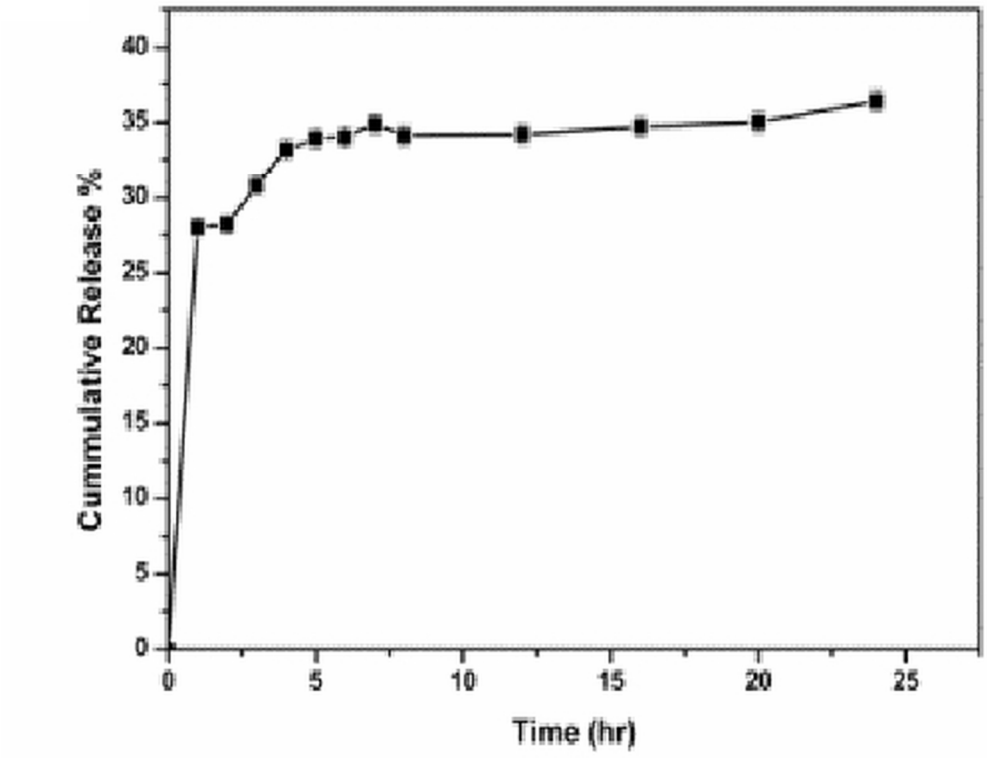


In-vitro release study of Lavender oil from PAN film for 24 h
105x82mm (300 x 300 DPI)

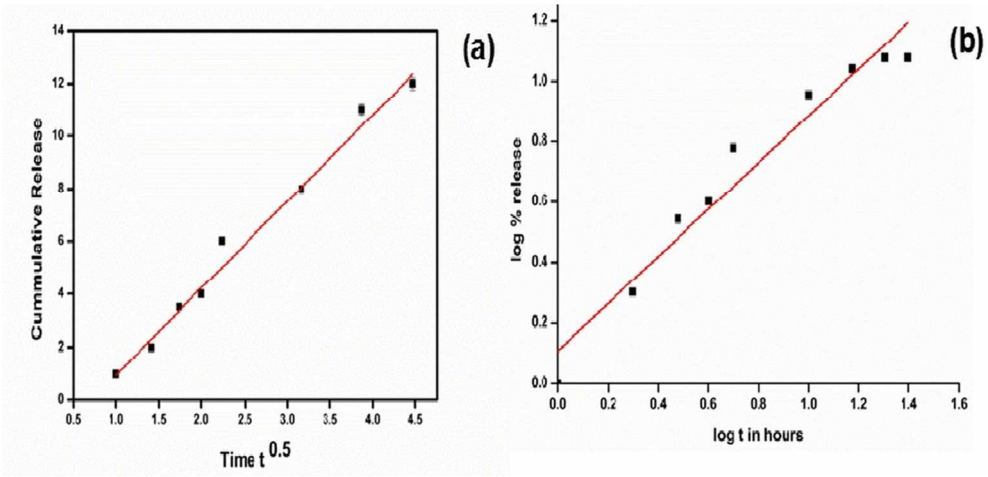


In-vitro release data fitted to (a) Higuchi model (b) Krosmeyer-Peppas model
107x50mm (300 x 300 DPI)

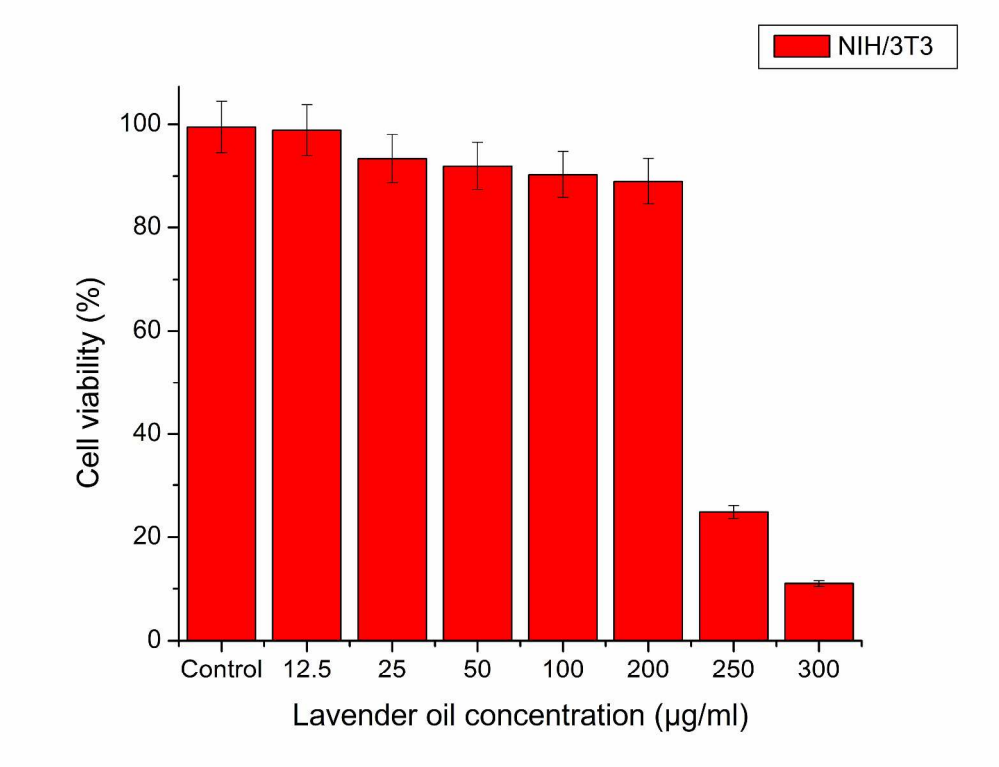


MTT Assay results of mouse fibroblast NIH/3T3 cells exposed to lavender oil at different concentrations
1746x1349mm (96 x 96 DPI)

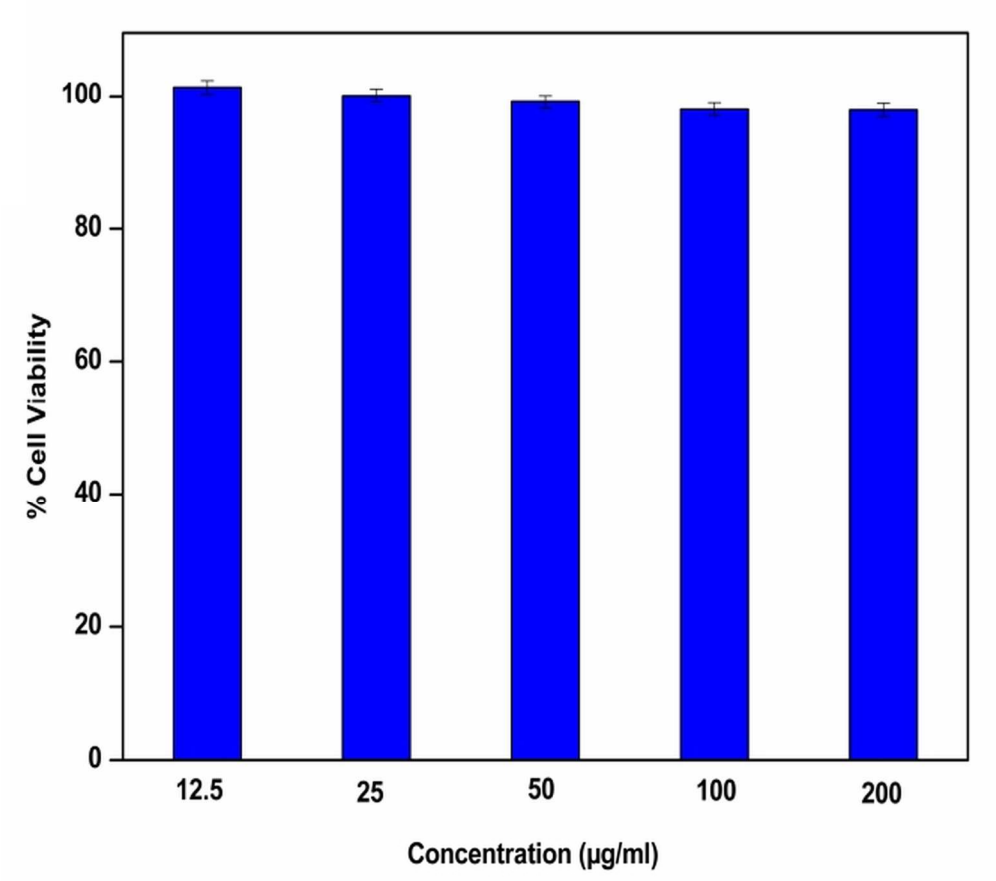


MTT assay results of mouse fibroblast NIH/ 3T3 cells to exposed to PAN blended with lavender oil at different concentrations
159x144mm (300 x 300 DPI)

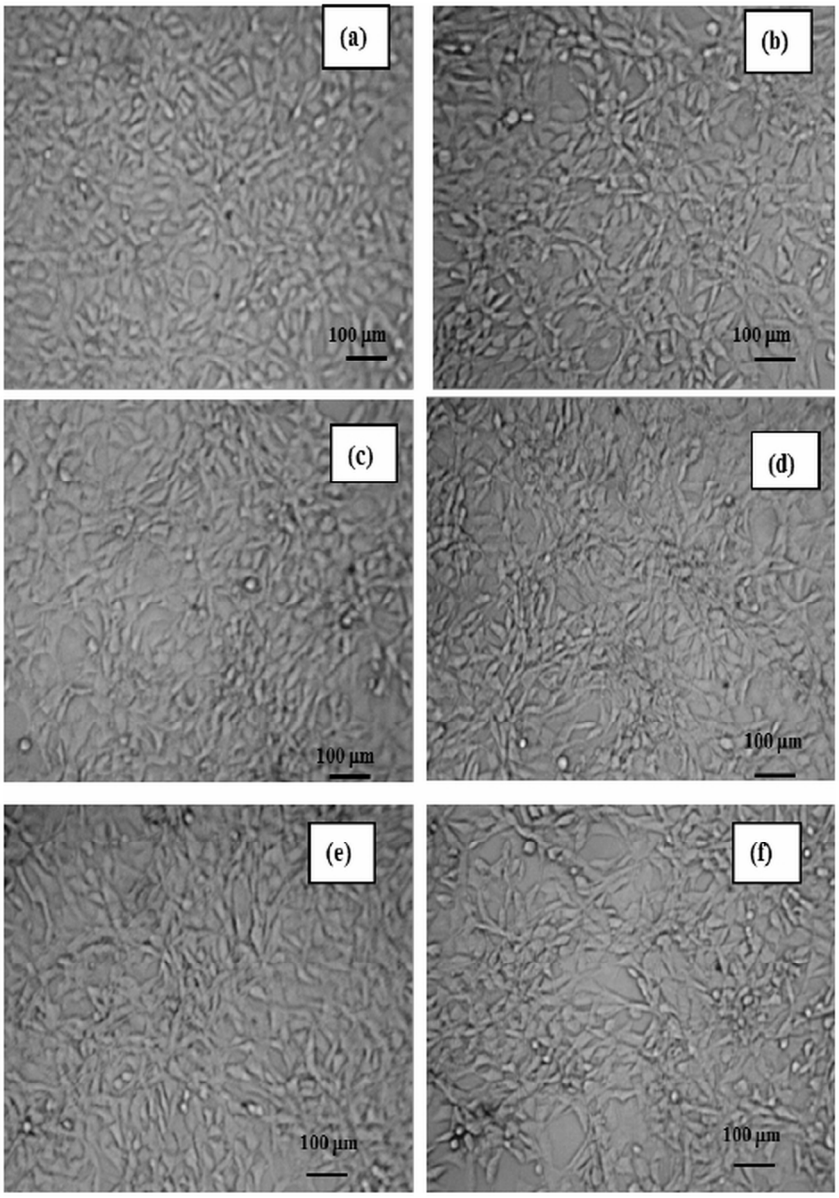


Photomicrograph of mouse fibroblast NIH/3T3 cell lines after treatment with samples at concentrations of lavender oil for 48 h (a) Control (b) 12.5 µg/mL (c) 25 µg/mL (d) 50 µg/mL (e) 100 µg/mL (f) 200 µg/mL.
201x285mm (300 x 300 DPI)